

Research on Passive Contaminant Transport in a Vegetated Channel

F. Jahra^{1*} and Y. Kawahara²¹*Oceanic Consulting Corporation, St. John's A1B 2X5, Canada*²*Department of Civil and Environment Engineering, Hiroshima University, Higashi-Hiroshima 739-8527, Japan*

Received 23 May 2015; revised 10 November 2015; accepted 19 November 2015; published online 04 March 2017

ABSTRACT. Vegetation plays an important role in the physical, ecological, and hydraulic functions of streams, rivers and many other water bodies and can affect the transport of water, sediment and nutrients both within the channel and to or between the riparian zones. This research studied the momentum and passive contaminant transport mechanism in a vegetated channel with a floodplain (river bank). Three dimensional numerical simulation and physical experimentations were conducted for turbulent flow in the presence of model vegetation. A non-linear $k-\epsilon$ model with a vegetation model for turbulent flow and an algebraic flux model proposed by Daly and Harlow (1970) (DH model) for contaminant transport were adopted. An in-house code developed by the authors was implemented for numerical simulations. Model vegetation zones were prepared in the channel to predict the mixing mechanism. The numerical results were compared with corresponding experimental observations. A good agreement between the simulated and experimental results was observed in terms of pollutant concentration.

Keywords: passive contaminant transport, non-linear $k-\epsilon$ model, algebraic flux model, vegetated channel

1. Introduction

Vegetation in streams and rivers has been considered as a source of flow resistance and a key factor for aquatic ecosystem and river management. In river hydrodynamics flow through aquatic vegetation is of high concern. Vegetation can occupy nearly every geomorphic position within the fluvial environment, see Figure 1. The presence of floodplain, i.e. river bank vegetation significantly affects the flow field in the main channel and enhances mass and momentum exchange between the main channel and the floodplain. Vegetation can affect the water quality by transporting sediment, and nutrients both within the channel and to or between the riparian zones. It also affects the contaminant transport in the fluvial environment. In recent years with the increase of environmental pollution the contaminant or pollutant transport in rivers has become an important topic in environmental hydraulics. There has been an increasing interest in predicting contaminant transport processes in compound channel flows for controlling pollution levels in rivers (Lin and Shiono, 1995). Numerical simulation as well as physical experiments on flow distribution and momentum transport in the presence of vegetation has been studied by many researchers in the last three decades e.g. Arnold et al. (1985), Shimizu and Tsujimoto (1994), Naot et al. (1996), Rameshwa-

ran and Shiono (2007), Kang et al. (2009), Sanjou et al. (2010), Jahra (2011). The impact of vegetation on pollutant or sediment transport is still an on-going research topic.

The flows in a compound channel (channel with floodplains) are characterized by complicated flow structure due to the presence of a shear layer at the interface between the main channel and the floodplain. Secondary currents of the second kind develop in prismatic channels due to the anisotropy of turbulence particularly near free surface and walls. During over-bank flows, the fast flow in the main channel is hindered by the comparatively slower floodplain flow causing generation of shear layer, secondary flow and large lateral momentum transfer. The presence of vegetation makes the flow pattern more complicated. The additional drag exerted by vegetation reduces the mean velocity, turbulence intensities and bed shear stress within a vegetated zone. This baffling promotes solute transport, sediment deposition and suppresses bed erosion. Arnold et al. (1985) measured the dye concentration in a compound channel and deduced the lateral mixing coefficient of the tracer. Wood and Liang (1989) conducted laboratory experiments to measure the tracer concentration and developed a two-dimensional semi-analytical model to predict tracer concentration in the open channel. Jaque and Ball (1995) experimentally studied the mixing of pollutant concentrations in a compound channel. Lin & Shiono (1995) performed numerical simulation for the channel without floodplains using both linear and non-linear $k-\epsilon$ models and concluded that the tracer concentration predicted by the non-linear $k-\epsilon$ model gives better agreement with measurements than that of the linear $k-\epsilon$ model. Shiono et al. (2003) carried out their research on solute transport through both the

* Corresponding author. Tel.: +1 709 7496118; fax: +1 709 7229064.
E-mail address: jahra.fatima@oceaniccorp.com (F. Jahra).



Figure 1. Natural river and channel with vegetation.

laboratory experiments and numerical simulations in a channel without vegetation. For numerical simulation these researchers adopted a non-linear $k-\varepsilon$ model, and predicted the solute transport with an eddy diffusivity model in an asymmetric compound channel, e.g. the experimental flume had its floodplain at only one side. Kang et al. (2009) investigated the characteristics of solute transport in a rectangular open channel without any floodplain with submerged vegetation.

Until now the characteristics of passive contaminant transport has not been discussed in detail for different types of vegetation arrangements on the banks of a compound channel. Thus, the need to predict the flow and transport of pollutant, sediment and nutrients in the presence of vegetation leads to laboratory experiments and numerical computations. The objective of present research is to investigate the characteristics of pollutant transport in a channel with a floodplain with different vegetation layouts through physical experiments and numerical computations and to propose a numerical model that reasonably predicts well the contaminant transport in presence of river-bank vegetation. The $k-\varepsilon$ model is the most commonly used two-equation model and has been used in a wide variety of problems in hydraulic and environmental engineering. The non-linear $k-\varepsilon$ model can simulate secondary currents successfully in compound channel flows by taking into account normal stress anisotropy. In the present research all numerical computations were conducted by a non-linear $k-\varepsilon$ model with a vegetation model, coupled with a scalar flux model (eddy diffusivity model) and an algebraic flux model (DH model) for predicting solute transport phenomena. As a representation of pollutant or contaminant solute, NaCl solution was used in this research.

2. Methodology

The flow and solute concentration measurements in a channel with a floodplain, i.e. compound channel were conducted by the authors. Experiments were carried out in the Hydraulic Engineering Laboratory of Hiroshima University, Japan. The

length, width and slope of the experimental flume are 2,200 cm, 182 cm and 1/500, respectively. The length-width ratio is 1:12. The channel has closed water supply system. Water is transported from downstream reservoir to the upstream reservoir by means of pipeline. In the flume there is an electric motor driven tailgate to obtain the uniform flow by adjusting the water surface slope through raising or lowering the tailgate. The floodplains were constructed on either side of the channel, having a height of 4 cm and a width of 45.5 cm. Model vegetation was planted over one floodplain as shown in the figures below. The vegetation was idealized with wooden rigid cylinders of 0.3 cm diameter and 5 cm height. The measurements were carried out with two types of vegetation zones prepared over one side of the floodplain as shown in Figure 2: (a) Case A1 - the floodplain fully covered by model vegetation; and (b) Case A2 - a 10 cm wide vegetation belt located along the junction of the main channel and the floodplain. Cross sectional layouts of the two types of vegetation and the flume photo are shown in Figure 3 and Figure 4, respectively. Three mean velocity components were measured by two-component electromagnetic current meters, L-type probe for streamwise, u -velocity and vertical, w -velocity components and I-type probe for spanwise v -velocity component. Water depth was measured by water level gauges at the frequency of 10 Hz. The probes of electromagnetic current meters are 0.3 cm diameter and 1.6 cm height. The electromagnetic field generated by the probe was not affected by the model vegetation stems as the distance between the probe and the adjacent model vegetation was large enough, 3cm by 3cm and the probe was located at the center of the 4 vegetation stems. Sodium Chloride, NaCl was used as tracer in the solute transport experiments and its concentration was measured by a densitometer with a probe of 0.2 cm diameter. NaCl was injected continuously at $x = 900$ cm, just below the free surface ($z = 7.9$ cm) with a 0.3 cm diameter nozzle. The solution injection locations were $y = 91$ cm, 136 cm, 138 cm and 148 cm (noted in Table 1). The solution was injected at each location for each experiment; for example, in Case A1-S1, so-

lution was injected at $x = 900$ cm, at the center of the channel ($y = 91$ cm) and the detail measurements of solute concentration were carried on along the section $x = 1000$ cm and 1100 cm, i.e. streamwise 100 cm and 200 cm away from the injection point. The discharge in the flume was $Q = 30$ L/s. The Froude number was 0.07 for Case A1 and 0.08 for Case A2 (considering flume width and mean flow velocity). The initial concentration of solute was 1% . Solute was dissolved in water and diluted by alcohol to set the injected mixture density the same as the flume water density at the working temperature (22 °C). The solute injection flow rate was 3 mL/s. The red dotted lines in Figure 2 indicate the measurement sections. Table 1 demonstrates the injection locations and the experimental conditions. To observe the solute spread pattern flow visualization was carried out through dye injection process shown in Figure 4. Aniline blue was used as the tracer dye.

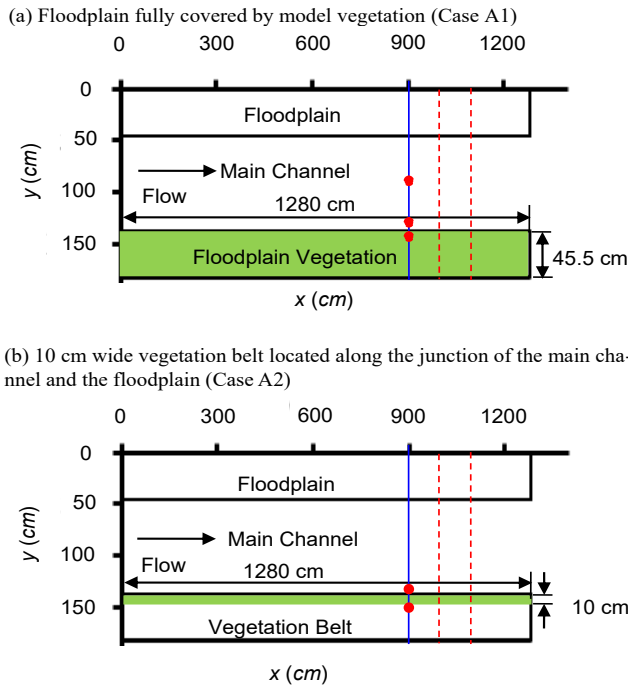


Figure 2. Vegetation placement and solution injection points (plan view). (The red dot shows the locations of the injection points in the y -direction).

Table 1. Experimental Condition for Solute Transport

Test case	Sub testcase	Water depth (cm)	Solute injection location			Injection flow rate (mLs ⁻¹)
			x (cm)	y (cm)	z (cm)	
A1	S1	8.0	900	91	7.9	3.0
	S2			136		
	S3			138		
A2	S4	7.9	900	136	7.8	3.0
	S5			148		

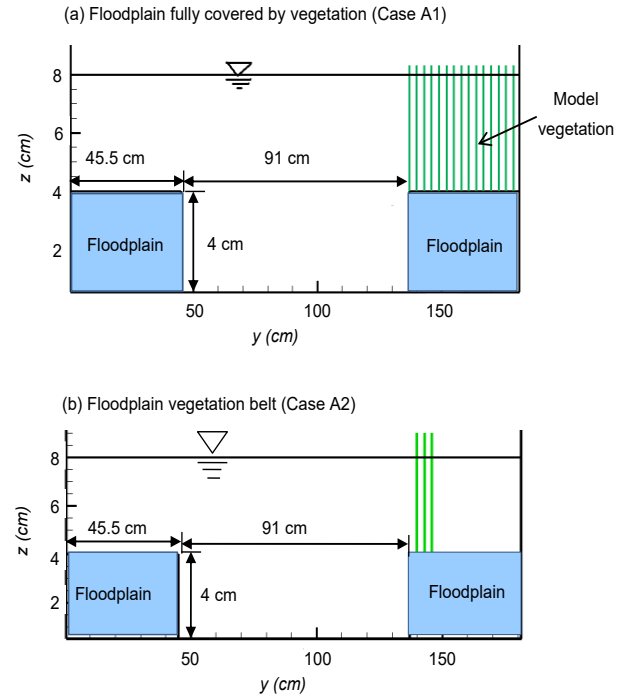


Figure 3. Vegetation placements in the experimental flume.

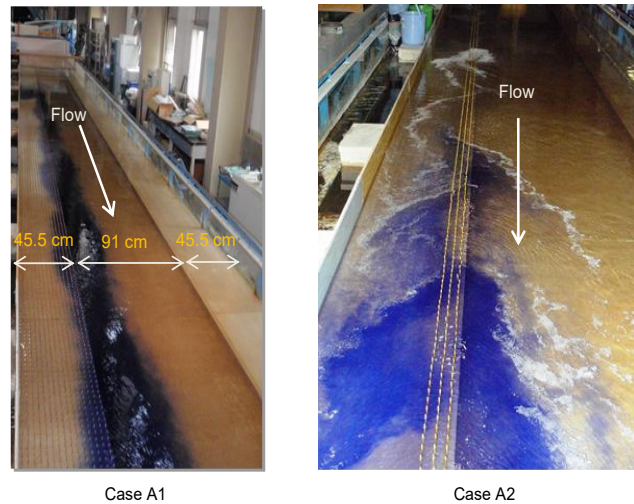


Figure 4. Photograph of dye spreading in the experimental flume.

3. Mathematical Formulations

3.1. Turbulence Model

Numerical simulations were conducted using a non-linear $k-\epsilon$ model. The computer code calculates hydrodynamics for three-dimensional flow field. The double averaged continuity and momentum equations were used for the numerical computation of turbulent flows in presence of vegetation zones (Jahra, 2011). The basic equations are:

$$\frac{\partial \langle \bar{u}_i \rangle}{\partial x_i} = 0 \quad (1)$$

$$\begin{aligned} \frac{\partial \langle \bar{u}_i \rangle}{\partial t} + \frac{\partial \langle \bar{u}_i \rangle \langle \bar{u}_j \rangle}{\partial x_j} + \frac{\partial}{\partial x_j} \left(\langle \bar{u}_i' u_j' \rangle + \langle \bar{u}_i' \bar{u}_j' \rangle \right) \\ = g_i - \frac{1}{\rho} \frac{\partial \langle \bar{p} \rangle}{\partial x_i} + \nu \frac{\partial^2 \langle \bar{u}_i \rangle}{\partial x_j \partial x_j} - \frac{1}{\rho} \frac{\partial \langle \bar{p} \rangle}{\partial x_i} + \nu \left\langle \frac{\partial^2 \bar{u}_i}{\partial x_j \partial x_j} \right\rangle \end{aligned} \quad (2)$$

Here, the over bar stands for time averaged, single prime for the deviation from the time average, angle brackets for the spatial average, and double primes for the deviation from the spatial average. The last two terms on the right hand side of momentum equation representing the pressure and viscous drag forces are modeled as follows:

$$-\frac{1}{\rho} \frac{\partial \langle \bar{p} \rangle}{\partial x_i} + \nu \left\langle \frac{\partial^2 \bar{u}_i}{\partial x_j \partial x_j} \right\rangle = -\frac{1}{2} C_D \lambda U_i \sqrt{U_j U_j} = -F_i \quad (3)$$

Here, p is the pressure, ρ is the density of water, F is the drag force exerted due to vegetation, C_D is the drag coefficient ($= 1.1$) and λ ($= 0.033$) is the vegetation density defined by $\lambda = D/l_x l_y$. D is the diameter of the vegetation stem and l_x and l_y are the adjacent vegetation distances in the x and y directions, respectively. Hereafter upper case for double-averaged velocity as $\langle \bar{u}_i \rangle = U_i$ for brevity is used. The Reynolds stress term and the velocity correlation term in the momentum equation are modeled as:

$$\begin{aligned} -\langle \bar{u}_i \bar{u}_j + \bar{u}_i' \bar{u}_j' \rangle &\equiv -\bar{u}_i \bar{u}_j \\ &= \nu_i S_{ij} - \frac{2}{3} k \delta_{ij} - \frac{k}{\varepsilon} \nu_i \sum_{\beta=1}^3 C_{\beta} \left(S_{\beta ij} - \frac{1}{3} S_{\beta \alpha \alpha} \delta_{ij} \right) \end{aligned} \quad (4)$$

$$\nu_i = C_{\mu} \frac{k^2}{\varepsilon} \quad (5)$$

$$S_{1ij} = \frac{\partial U_i}{\partial x_m} \frac{\partial U_j}{\partial x_m}, \quad S_{2ij} = \frac{1}{2} \left(\frac{\partial U_m}{\partial x_i} \frac{\partial U_j}{\partial x_m} + \frac{\partial U_i}{\partial x_m} \frac{\partial U_m}{\partial x_j} \right), \quad (6)$$

$$S_{3ij} = \frac{\partial U_m}{\partial x_i} \frac{\partial U_m}{\partial x_j}$$

$$S = \frac{k}{\varepsilon} \sqrt{\frac{1}{2} S_{ij} S_{ij}}, \quad \Omega = \frac{k}{\varepsilon} \sqrt{\frac{1}{2} \Omega_{ij} \Omega_{ij}}, \quad (7)$$

$$S_{ij} = \frac{\partial U_i}{\partial x_j} + \frac{\partial U_j}{\partial x_i}, \quad \Omega_{ij} = \frac{\partial U_i}{\partial x_j} - \frac{\partial U_j}{\partial x_i}$$

$$C_{\mu}(M) = \min \left[0.09, \frac{0.3}{1 + 0.09 M^2} \right], \quad M = \max(S, \Omega) \quad (8)$$

$$C_1 = 0.4 \times f(M), \quad C_2 = 0, \quad C_3 = -0.13 \times f(M) \quad (9)$$

$$f(M) = 1 / (1 + 0.01 M^2) \quad (10)$$

where ν_i is the eddy viscosity. The Equations (11) and (12) below represent k and ε , are the double-averaged turbulent kinetic energy and its dissipation rate, respectively. C_{μ} has been computed using the formula proposed by Kimura & Hosoda (2003). A detailed expression of the above equation can be found in Jahra (2011).

The transport equations for k and ε are written as:

$$\frac{\partial k}{\partial t} + \frac{\partial U_j k}{\partial x_j} = \frac{\partial}{\partial x_m} \left[\left(\frac{\nu_i}{\sigma_k} + \nu \right) \frac{\partial k}{\partial x_m} \right] + P_{rod} + S_k - \varepsilon \quad (11)$$

$$\begin{aligned} \frac{\partial \varepsilon}{\partial t} + \frac{\partial U_j \varepsilon}{\partial x_j} \\ = \frac{\partial}{\partial x_m} \left[\left(\frac{\nu_i}{\sigma_{\varepsilon}} + \nu \right) \frac{\partial \varepsilon}{\partial x_m} \right] + \frac{\varepsilon}{k} C_{\varepsilon 1} P_{rod} + S_{\varepsilon} - C_{\varepsilon 2} \frac{\varepsilon^2}{k} \end{aligned} \quad (12)$$

$$P_{rod} = -u_i u_j \frac{\partial U_i}{\partial x_j} \quad (13)$$

The double-averaging concept introduces source and sink terms, S_k and S_{ε} , into the transport equations for k and ε , which was originally proposed by Green (1992) and modified by the authors (Jahra et al. 2010):

$$\begin{aligned} S_k &= F_i U_i - 2 C_D \lambda \sqrt{U_i U_i} \\ S_{\varepsilon} &= \frac{3}{2} \frac{\varepsilon}{k} F_i U_i - 1.4 C_D \lambda \sqrt{U_i U_i} \varepsilon \\ \sigma_k &= 1.0, \quad \sigma_{\varepsilon} = 1.3, \quad C_{\varepsilon 1} = 1.44, \quad C_{\varepsilon 2} = 1.92 \end{aligned} \quad (14)$$

The computer code was developed in-house by the authors. The basic equations were discretized by the Finite Volume method and the SIMPLE algorithm (Patankar, 1980) was implemented for pressure-velocity coupling. For unsteady terms, a fully implicit scheme was used. The QUICK (Quadratic Upstream Interpolation for Convective Kinematics) scheme proposed by Leonard, 1979 was applied to the convection terms and the central differencing scheme was used for the diffusion terms in the momentum equations. The k and ε equations were discretized by a Power-law scheme. Along the bottom and the side walls a "wall function" technique were applied. The near free surface turbulent dissipation rate was specified as follows:

$$\varepsilon_s = C_{\mu}^{3/4} k_s^{3/2} / (0.4 \times \Delta Z_s) \quad (15)$$

where the suffix s indicates the value at the point adjacent to the free surface and ΔZ_s is the normal distance from the free surface.

3.2. Passive Contaminant Transport Model

The concentration of a passive scalar can be computed by solving the following transport equation:

$$\frac{\partial C}{\partial t} + \frac{\partial U_j C}{\partial x_j} = \alpha \frac{\partial^2 C}{\partial x_j \partial x_j} - \frac{\partial}{\partial x_j} (\overline{u_j C}) \quad (16)$$

where C is the scalar concentration, α is the molecular diffusivity of the scalar = 1.612×10^{-5} (cm²/s) for NaCl at 25 °C temperature and $\overline{u_j C}$ is the scalar flux composed of turbulent flux and the correlation between deviated velocity and concentration from their spatial averages. The parameter $\overline{u_j C}$ should be modeled.

(1) Isotropic Eddy Diffusivity Model

The simplest model for turbulent scalar fluxes follows from the standard gradient-diffusion hypothesis (SGDH), where the turbulent scalar flux is assumed proportional to the mean scalar gradient as follows. This model entails the concept of eddy diffusivity to estimate the scalar flux:

$$\overline{u_j C} = -D_t \frac{\partial C}{\partial x_j}, D_t = \frac{\nu_t}{\sigma_c} \quad (17)$$

where D_t = eddy diffusivity for scalar, and σ_c the turbulent Schmidt number (= 1.0).

(2) Algebraic Flux Model (DH Model)

The algebraic models evaluated in the present work are formulated starting from the exact transport equation of the scalar fluxes $\overline{u_j C}$. Daly and Harlow (1970) introduced an eddy diffusivity tensor proportional to the Reynolds stress for the scalar flux. The DH model represents an algebraic flux model and gives a general form of the flux vector as a linear combination of the Reynolds stress:

$$\overline{u_j C} = -1 \cdot C_c \tau_c u_j u_m \frac{\partial C}{\partial x_m} \quad (18)$$

where C_c is the model parameter (= 0.4) and, τ_c is the characteristic time-scale = k/ε . Zero-flux condition is applied along the boundaries. The concentration at the injection point is specified.

4. Discussion

The non-linear $k-\varepsilon$ turbulence model coupled with an eddy diffusivity model and a DH model for solute transport was first validated against the experimental data published in Shiono et al. (2003). It is seen that the DH model reproduces a reasonable agreement with the measurements (Jahra, 2011). The turbulent flow model was validated against different flow fields in the previous studies (Jahra et al., 2010, 2011). The following sections contain a brief discussion of the calculated results and the respective experimental data obtained from contaminant transport study.

4.1. Floodplain Fully Covered by Model Vegetation: Case A1

The laboratory experiments were carried out for three dif-

ferent cases based on solution injection points described in Table 1. In Case A1 where the floodplain is fully covered by the model vegetation, solution of NaCl was injected at three different locations for three different sub-cases, i.e. in Case A1-S1 the NaCl solution was injected at the center of the channel ($y = 91$ cm); In Case A1-S2, in the main channel, near the interface of the main channel and the vegetated floodplain ($y = 136$ cm) and in Case A1-S3, within the vegetation zone, near the junction point ($y = 138$ cm). Figure 5(a) shows the channel's sectional view of contours of measured solute concentration distribution 100 cm away from the injection point. In this case salt water was injected at the middle of the channel at $y = 91$ cm. The measured result is compared with the calculated results by both the solute transport models. The comparison between the experimental result and numerical one by ED model shows apparent difference in the shape of contours. The measured contours show wider and less deep spread than calculated one. On the contrary DH model shows comparatively better agreement with the measured result. Figure 6 shows the lateral distribution of non-dimensional solute concentration near the free surface at the sections $x = 1,000$ cm and $1,100$ cm, respectively. The measurement points are located just below the water surface, at 7.5 cm above the channel bed. In the figures C_0 represents the initial solute concentration. In the figure a comparison had been made between the experimental data and the simulation results by DH model. A good agreement was observed. The DH model takes into account the anisotropy of turbulence, i.e. it incorporates the secondary currents and shows a reasonable agreement with the measured result. The spread of solute is mainly attributed to the convection due to the secondary currents and turbulent diffusion. The flow direction of secondary currents mainly determines the distribution of solute. This can be identified in Figure 5 where the peak of the solute concentration was shifted a little from the center of the main channel towards the vegetated floodplain, located at the right side of the flow direction (and the figures). Figure 5(b) shows the calculated solute distribution by ED model and the secondary flow distribution. It is found that the secondary currents direct towards the vegetated floodplain near the water surface and in a reverse way near the bed. However the magnitude of secondary flow is too small to reproduce the measured results quantitatively. The effect of secondary current is more evident in the other case studies (Case S2-S5). In Case A1-S1 the peak of the solute concentration was not laterally shifted much from the injection point due to diminutive secondary currents in the main channel, shown in Figure 5 (b).

In Case S2 NaCl solution was injected at $y = 136$ cm, which is located in the main channel, near the interface of the main channel and the vegetated floodplain. Figure 2(a) shows all the solute injection locations of Case A1 (S1-S3). Figure 7 shows cross sectional contour distributions comparing the experimental and the simulation result at $x = 1,000$ cm. It can be observed that the concentration peak was shifted to the vegetated floodplain and the high concentration region was shifted more in the measured results relative to the calculated ones. The arrow above the free surface indicates the spreading direction of so-

lute concentration and “•” expresses the exact point of solute injection. The secondary cell with clockwise rotation over the vegetated floodplain (Figure 7(b) and more clearly in Figure 8) plays the dominant role in transporting the solute within the cross-section. The solute of high concentration near the free surface is conveyed from the main channel to the floodplain whereas the solute of low concentration is transported from the floodplain to the main channel near the bed. Arnold et al (1985) measured the turbulent Schmidt number σ_c between 0.4-1.0. It implies that the use of σ_c less than 1.0 in the lateral direction and larger than 1.0 in the vertical direction leads to better agreement between the experimental and the calculated result with the isotropic eddy diffusivity model. This indicates the need of a more refined flux model. It was observed in Figure 7(c) that DH model shows relatively better agreement with the measured result.

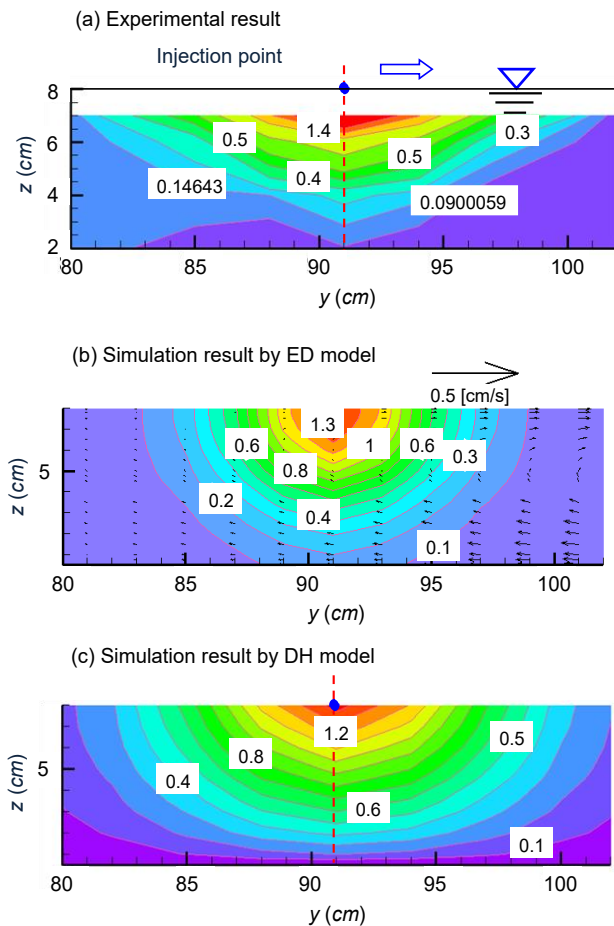


Figure 5. Contour of solute concentration $[C/C_0 \cdot 1,000]$ in Case S1 at $x = 1,000$ cm.

The same phenomenon can be observed in Case S3 for the solute injection point at $y = 138$ cm, which is located in the vegetated floodplain, near the interface of the main channel and the vegetation zone. Figure 9 shows the spanwise distribution of non-dimensional solute concentration of the experimental

and the simulation results at $x = 1000$ cm and $z = 7.5$ cm. In Cases S2 and S3 the shift of the peak of solute concentration is more noticeable compared to Case S1 due to strong secondary current cells. The generation of two secondary current cells over the vegetated floodplain and in the main channel near the vegetated floodplain contributes in solute spread in Cases S2 and S3. DH model shows better agreement with the measured one compared to ED model. In ED model the solute concentration remains at its injection point indicating its inability to compute the anisotropic phenomena where secondary currents are more pronounced.

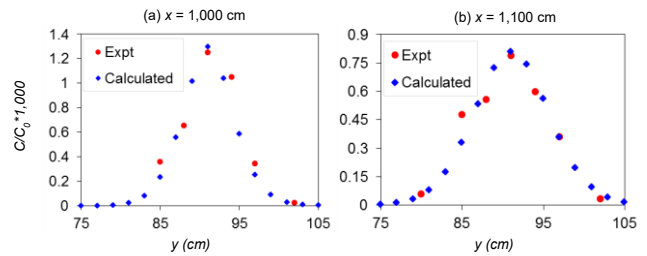


Figure 6. Distribution of solute concentration $[C/C_0 \cdot 1,000]$ across the center of the channel (Case S1).

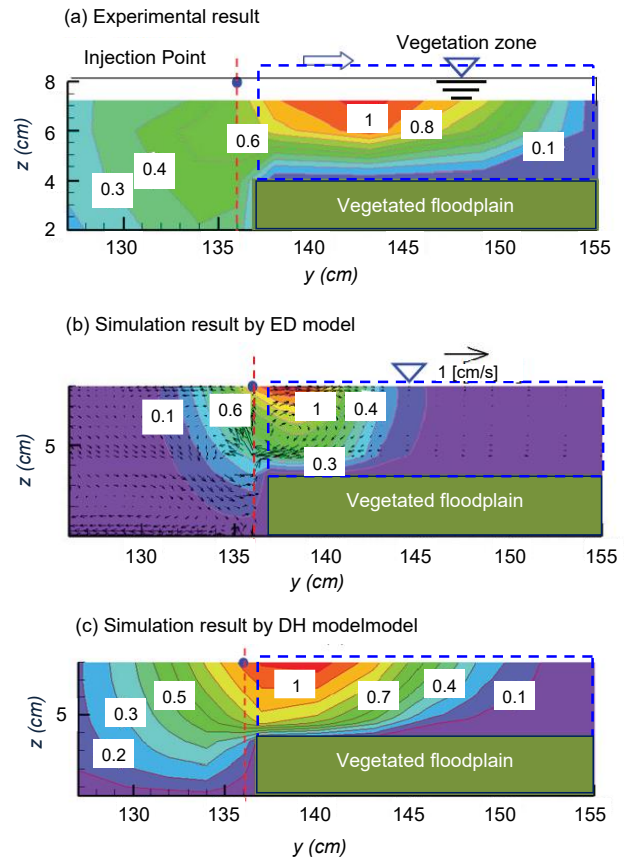


Figure 7. Contour of solute concentration $[C/C_0 \cdot 1,000]$ in Case S2 at $x = 1,000$ cm.

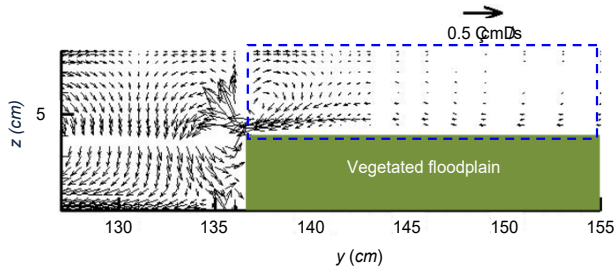


Figure 8. Secondary current, vw vector distribution (Case A1).

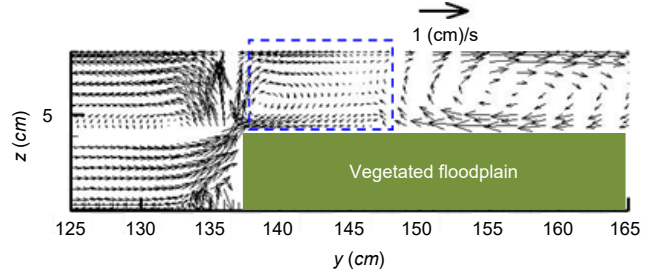


Figure 11. Secondary current, vw vector distribution (Case A2).

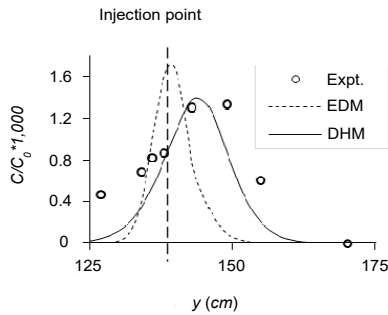


Figure 9. Spanwise distribution of solute concentration $[C / C_0 * 1,000]$ in Case S3 at $x = 1,000$ cm, $z = 7.5$ cm.

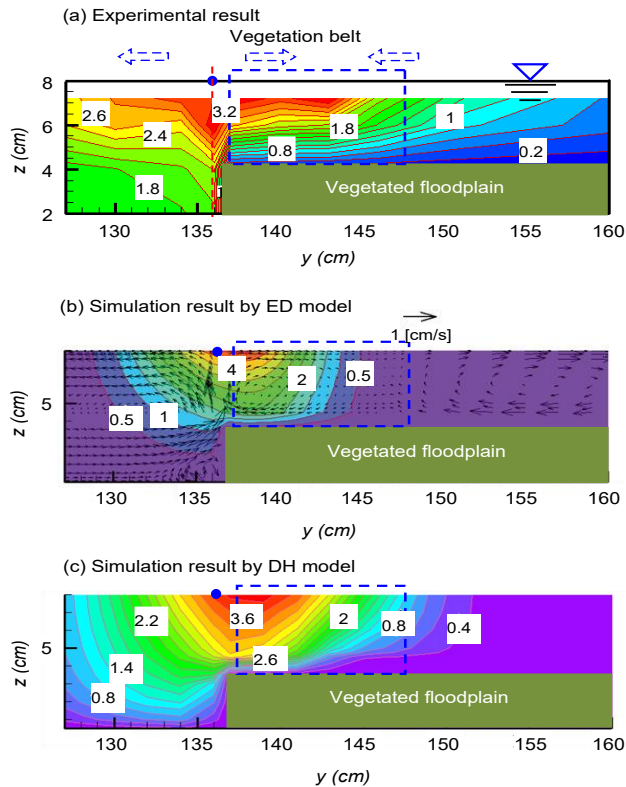


Figure 10. Contour of solute concentration $[C/C_0 * 1,000]$ in Case A2 at $x = 1,000$ cm.

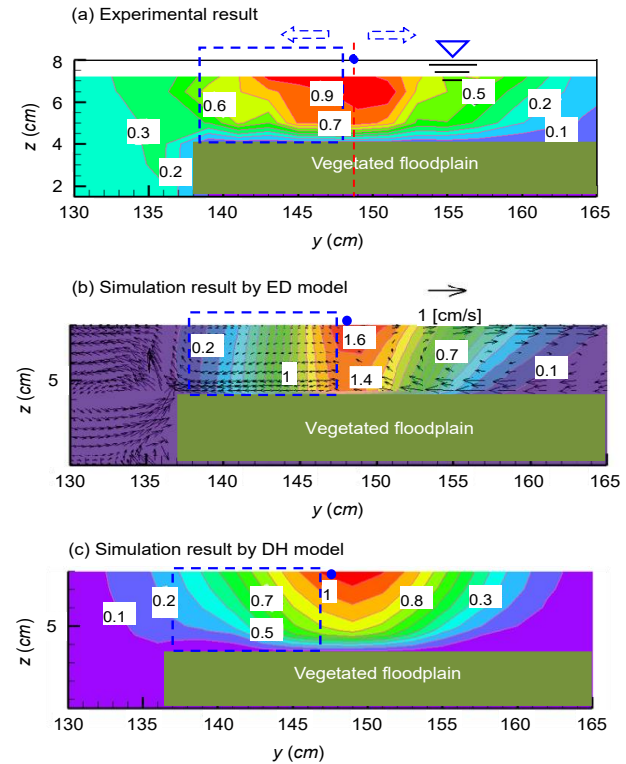


Figure 12. Contour of solute concentration $[C/C_0 * 1,000]$ in Case A2 at $x = 1,100$ cm. (a) experimental result, (b) simulation result by ED model, (c) simulation result by DH model.

4.2. Floodplain Vegetation Belt: Case A2

The solute concentration distribution is greatly affected by the presence of the vegetation belt over the floodplain located along the interface of the main channel and the floodplain. In Case A2 (floodplain with vegetation belt) salt water was injected at two points just below the free surface of the water at $y = 136$ cm (Case A2-S4) and $y = 148$ cm (Case A2-S5). The first point is located in the main channel, near the interface of the floodplain with vegetation belt. The second injection point is located just at the back side of the vegetation belt over the floodplain (Figure 2(b)). The eddy diffusivity model as well as the algebraic flux model was implemented to calculate the solute distribution.

Figure 10 describes the solute distribution when salt water was injected at $y = 136$ cm. It can be observed that both the simulation results underestimate the mixing in the span-wise direction. The magnitude of secondary flow in the calculated result by the $k-\epsilon$ turbulence model is too small to reproduce the measured results accurately. The secondary flow distribution is shown in Figure 10(b) (to relate with the solute distribution) and Figure 11. Complicated flow structure due to the vegetation belt (Case C5) can be observed here which affects not only the secondary current distribution but also creates large-scale turbulence (left photo of Figure 4). Weak clockwise secondary current cell generated within and at the right side of the vegetation belt (Figure 10(b) and more clearly in Figure 11) restricts the lateral mixing of the solute. In ED model turbulent Schmidt number is needed to be adjusted, but its isotropic nature restricts its applicability in complex flow field. On the contrary DH model, taking into account the anisotropy of turbulences gives better agreement with the measured data compared to the ED model. It is also inferred that for complicated flow situations the DH model parameter C_c that controls the scalar flux might need to be tuned for better agreement with the measurement.

Figure 12 shows the solute distribution where salt water was injected just at the right side of the vegetation belt at $y = 148$ cm (Case A2-S5). The concentration of the solute was spread within and towards the right side of the vegetation belt due to the distribution of secondary currents. The high concentration zone is shifted towards the right side due to the generation of strong secondary current cell at the right side of vegetation belt. The performances of ED model and DH model against experimental result are shown in Figures 12 (b) and 12(c). The DH model shows better agreement. ED model underestimates the solute mixing in the lateral direction and over estimates in the vertical direction.

The present model has shown good performance against the experimental data of Shiono et al. (2003) as secondary current is strong and the flow pattern was less complicated due to the absence of floodplain vegetation. It is noted that comparison between the experimental and the calculated results gives an impression that the measured data of this study may have some inaccuracies, which may be due to the larger solute density than the flume water due to the evaporation of alcohol with time. Thus it is found that the algebraic flux model gives better agreement with the measurement by taking into account of the anisotropic process of turbulent diffusion. For the above calculated results it can be concluded that the calculated results can be improved by implementing special free surface damping effect in the present non-linear $k-\epsilon$ model. Accurate calculation of free surface secondary currents will lead better agreement with the experimental results. There is a scope to improve the passive contaminant transport model.

5. Conclusions

Flume experiments were carried out for turbulent open channel flows in the presence of the floodplain vegetation under emergent conditions. NaCl solution was injected in the flume to observe the contaminant transport characteristics in pre-

sence of vegetation. Numerical simulations were performed with a non-linear $k-\epsilon$ model coupled with a vegetation model together with an eddy diffusivity model and an algebraic flux model to discuss the contaminant transport in presence of vegetation. This research will be beneficial for revealing the contaminant transport behavior in the fluvial environment in presence of river bank vegetation and will be useful for pollution control in the river environment.

Through comparisons between the calculated results and the measured data by the authors it can be inferred that

- Solute concentration is reasonably predicted by the non-linear $k-\epsilon$ model. The algebraic flux model proposed by Daly and Harlow, takes into account the anisotropy of turbulence and gives better agreement with measured solute concentration distribution compared to the isotropic eddy diffusivity model. The isotropic eddy diffusivity underestimates scalar fluxes, leading to discrepancy with the measured results in complex flow fields.
- The vegetation model proposed by the authors predicts the solute transportation characteristics in presence of vegetation reasonably well.
- Secondary currents generated near the free surface enhance the shifting of solute concentration peak from the main channel towards the vegetated floodplain.
- It is necessary to tune the model parameters, the turbulent Schmidt number σ_c for ED model and C_c for DH that controls the scalar flux for better prediction of solute transport phenomenon.
- It is also useful to refine the turbulence model to more accurately predict secondary current flows which play an important role in solute transfer process.

The present non-linear $k-\epsilon$ model has the weak point that here free surface is treated as a symmetry plane. So damping effect must be introduced to calculate secondary currents at the free surface accurately. Predicting secondary currents near the free surface will lead to better agreement between the experimental results and the calculated one.

Acknowledgements: The authors would like to thank the Government of Japan for providing the first author the MEXT Scholarship, which made this study possible. The corresponding author would also like to express her gratitude to the *Oceanic Consulting Corporation* for support in publishing this research as an article.

References

- Arnold, U., Pasche, E., and Rouve, G. (1985). Mixing in river of compound cross section, *Proc. 21st IAHR Congress*, Melbourne, Australia, pp. 168-172.
- Daly, B.J. and Harlow, F.H. (1970). Transport equations in turbulence. *Phys. Fluids*, 13, 2634-2649. <http://dx.doi.org/10.1063/1.1692845>
- Green, S.R. (1992). Modelling turbulent air flow in a stand of widely-spaced trees. *Phoenics J.*, 5(3), 294-312.
- Jahra, F., Yamamoto, H., Hasegawa, F., and Kawahara, Y. (2010). Mean flow and turbulence structure in meandering open channel flows with submerged and emergent vegetation, *Proc. Int. Confe-*

- rence on Fluvial Hydraulics (*RiverFlow 2010*), Braubuschweig, Germany, 1, 153-161.
- Jahra, F. (2011). *Effect of vegetation on flow structure and mass transfer in open channels*, Ph.D Dissertation, Department of Civil and Environmental Engineering, Hiroshima University, Japan.
- Jahra, F., Kawahara, Y., and Hasegawa, F. (2011). Numerical simulation of turbulent flow in a partially vegetated open channel. *Annu. J. Hydraul. Eng. JSCE*, 55, 193-198.
- Jaue, D.T. and Ball, J.E. (1995). Mixing of pollutant concentrations in a compound channel, *Proc. 26th IAHR Congress*, London, UK, Vol. A, pp. 57-62.
- Kimura, I. and Hosoda, T. (2003). A non-linear k- ϵ model with realizability for prediction of flows around bluff bodies. *Int. J. Numer. Meth. Fluids*, 42(8), 813-837. <http://dx.doi.org/10.1002/flid.540>
- Kang, H., Choi, S.K., and Choi, B. (2009). Solute transport in open-channel flows with submerged vegetation, *33rd IAHR Congress: Water Engineering for a Sustainable Environment*, Vancouver, Canada, pp. 1890-1899.
- Leonard, B.P. (1979). A stable and accurate convective modelling procedure based on quadratic upstream interpolation. *Comput. Meth. Appl. Mech. Eng.*, 19(1), 59-98. [http://dx.doi.org/10.1016/0045-7825\(79\)90034-3](http://dx.doi.org/10.1016/0045-7825(79)90034-3)
- Lin, B. and Shiono, K. (1995). Numerical modelling of solute transport in compound channel flows. *J. Hydraul. Res.*, 33(6), 773-788. <http://dx.doi.org/10.1080/00221688909498551>
- Naot, D., Nezu, I., and Kakagawa, H. (1996). Hydrodynamic behavior of partly vegetated open-channels. *J. Hydraul. Eng.*, 122(11), 625-633. [http://dx.doi.org/10.1061/\(ASCE\)0733-942](http://dx.doi.org/10.1061/(ASCE)0733-942)
- Patankar, S.V. (1980). *Numerical Heat Transfer and Fluid Flow*, Hemisphere.
- Rameshwaran, P. and Shiono, K. (2007). Quasi two-dimensional model for straight overbank flows through emergent vegetation on floodplains. *J. Hydraul. Res.*, 45(3), 302-315. <http://dx.doi.org/10.1080/00221686.2007.9521765>
- Sanjou, M., Nezu, I., Suzuki, S., and Itai, K. (2010). Turbulence structure of compound open-channel flows with one-line emergent vegetation, *9th International Conference of Hydrodynamics*, Shanghai, China, pp. 577-581. <http://dx.doi.org/10.1201/b10553-38>
- Shimizu, Y. and Tsujimoto, T. (1994). Numerical analysis of turbulent open-channel flow over a vegetation layer using a k- ϵ turbulence model. *J. Hydrosci. Hydraulic Eng.*, 11(2), 57-67.
- Shiono, K., Scott, C.F., and Kearney, D. (2003). Prediction of solute transport in a compound channel using turbulence models. *J. Hydraul. Res.*, 41(3), 247-258. <http://dx.doi.org/10.1080/00221680309499970>
- Wood, I.R. and Liang, T. (1989). Dispersion in an open channel with a step in the cross-section. *J. Hydraul. Res.*, 27(5), 587-601. <http://dx.doi.org/10.1080/00221688909499112>